

1-1-1960

Correlation between tensile creep and flexural creep of alpha uranium at room temperature

Stephen Nathaniel Falken
Iowa State University

Follow this and additional works at: <https://lib.dr.iastate.edu/rtd>

 Part of the [Engineering Commons](#)

Recommended Citation

Falken, Stephen Nathaniel, "Correlation between tensile creep and flexural creep of alpha uranium at room temperature" (1960).
Retrospective Theses and Dissertations. 18412.
<https://lib.dr.iastate.edu/rtd/18412>

This Thesis is brought to you for free and open access by the Iowa State University Capstones, Theses and Dissertations at Iowa State University Digital Repository. It has been accepted for inclusion in Retrospective Theses and Dissertations by an authorized administrator of Iowa State University Digital Repository. For more information, please contact digirep@iastate.edu.

CORRELATION BETWEEN TENSILE CREEP AND FLEXURAL CREEP OF
ALPHA URANIUM AT ROOM TEMPERATURE

by

Stephen Nathaniel Falken

A Thesis Submitted to the
Graduate Faculty in Partial Fulfillment of
The Requirements for the Degree of
MASTER OF SCIENCE

Major Subject: Nuclear Engineering

Approved:

Signatures have been redacted for privacy

Iowa State University
Of Science and Technology
Ames, Iowa

1960

TABLE OF CONTENTS

	Page
I. INTRODUCTION.	1
II. REVIEW OF THE LITERATURE.	3
III. OBJECTIVES OF THE INVESTIGATION	6
A. Analytical Objective.	6
B. Experimental Objectives	6
IV. THEORETICAL DEVELOPMENT	8
A. The Creep Stress Distribution in a Beam	8
B. Predicting Flexural Creep Strain from Tensile Creep Strain.	15
V. PROCEDURE	22
A. General Procedure	22
B. Tensile Creep Tests	23
1. Material.	23
2. Apparatus	25
C. Flexural Creep Tests.	25
1. Material.	25
2. Apparatus	26
VI. EXPERIMENTAL RESULTS.	30
VII. DISCUSSION OF RESULTS	44
A. The Creep Curves.	44
B. The Ratio Curves.	49
C. The Prediction Equation	53
VIII. SUMMARY AND CONCLUSIONS	57
IX. TOPICS FOR FURTHER INVESTIGATION.	59
X. LITERATURE CITED.	60
XI. ACKNOWLEDGEMENTS.	62

I. INTRODUCTION

In recent years the efforts to understand the mechanism of creep and the factors which influence creep have been greatly intensified. The need for better creep resistant alloys to service the demands of a rapidly advancing technology has compelled the acquisition of a more fundamental knowledge of the creep phenomenon.

By far the most widely employed creep test has been the simple tension test. Relatively few investigations have been carried out with bending, torsion, or pressure as the stress state. Although the tensile creep test gives an indication of the relative creep resistance of materials, engineering design data for applications where the applied loads do not produce simple tension may not always be accurately obtained from this test. Thus there is a need for creep data to be obtained from other stress states, as well as for combinations of stress states.

An incident occurred several years ago which vividly illustrated the importance of properly designing for flexural creep. In 1955 the Mark II core of the EBR-1 reactor underwent a partial meltdown, which served to cast much doubt on the possibility of safely controlling fast power reactors (1, 2). Subsequent analysis of the core showed that the positive prompt temperature coefficient that was present which caused the meltdown was due solely to features in the engineering

design of the core. The fuel elements were rods of U^{235} clamped at the top and bottom. During reactor operation the side of each fuel rod closer to the center of the reactor became hotter than the side away from the center, due to the shape of the power generation curve. The thermal gradient set up in each rod caused the rod to bow, the inner side expanding relative to the outer side, and the middle of the fuel rod was pushed closer to the center of the reactor, causing an increase in reactivity. The bowing of the fuel rods is an example of flexural creep caused by thermal stress. The fuel assemblies in subsequent fast reactor cores have been made very rigid in order to reduce this bowing.

High temperature flexural creep tests are difficult to conduct. It would therefore be highly desirable if the flexural creep behavior of a material could be predicted from a knowledge of the tensile creep behavior, and it is to this end that this study is directed. Alpha uranium is an ideal material upon which to conduct such a study, in the sense that it exhibits plastic behavior at normal temperature and stress levels, thereby simulating the behavior of many other materials at high temperature and stress levels. This study is a vital step in the larger project of correlating creep induced by various stress states with simple tensile creep for all materials, and under a wide range of temperature and stress levels.

II. REVIEW OF THE LITERATURE

The first analysis of flexural creep was reported by McCullough in 1933 (3). The results of his experiments with lead beams demonstrated the linearity of strain with distance from the neutral axis; that is, plane sections remained plane even during creep. He proposed that the stress-minimum creep rate information obtained from ordinary tensile creep tests could be used to predict the stress distribution in a beam during creep.

Tapsell and Johnson (4), also experimenting with lead beams, demonstrated in 1935 that plane sections remained plane during flexural creep; that the initial linear stress distribution became completely redistributed within twelve minutes to a creep stress distribution, which thereafter remained constant with time; and that the creep rate in any fiber was approximately equal to the creep rate produced by a pure tensile stress equal in magnitude to the flexural stress at the fiber. They also showed that the redistributed stress in the outer fiber of the beam is $\frac{2n + 1}{3n}$ the elastic stress, where n is the slope of the creep rate-tensile stress curve plotted on log paper. The work of Tapsell and Johnson is considered to be the classical work on flexural creep.

Marin and Zwissler (5), creep testing beams of aluminum, observed discrepancies between the observed minimum creep

rates in flexure and the flexural creep rates calculated on the basis of tensile creep tests, in which a linear dependence of creep strain on time and a power relation between minimum creep rate and stress were assumed. The discrepancies were due to the fact that both the tensile and flexural creep curves departed considerably from the assumed linear dependence on time.

Marin and Cuff (6) reported essentially the same situation in attempting to correlate the tensile and flexural creep behavior of the plastic polystyrene. The minimum creep rate, assumed related to the applied stress by the power law $\dot{\epsilon} = B\sigma^n$, was obtained from tensile creep tests performed at low stresses for a period of 1000 hours. Findley (7) has shown that the power law is unsatisfactory for polystyrene at low stresses, and Gohn (8) has shown that, for the plastic polyethylene, as well as for many metals, the minimum creep rates are seldom obtained from tests of such short duration.

Popov (9) examined the stress distribution in a beam during creep by applying an approximate summation procedure to small increments of stress and time. In this way he was able to obtain the stress distribution in a beam at any time, even during the transient period prior to the steady state condition, which Tapsell and Johnson were not able to do. Popov applied his unique method to the calculation of the creep deflection of an imaginary copper beam, but did not report

any experimental verification.

Pao and Marin (10) presented an analysis of the flexural creep of plexiglass. They found that an accurate correlation between tensile and flexural creep was hampered by the fact that the creep rates in both cases continually decreased with time, instead of varying linearly as assumed.

Findley and Poczatek (11) studied the creep deflections of beams of canvas laminate. They assumed a continually decreasing creep rate in tension, and assumed the relationship between tensile creep strain (ϵ_T), time (t), and stress (σ) to be of the form

$$\epsilon_T = \left(\epsilon'_0 + m' t^a \right) \sinh \frac{\sigma}{\sigma_0}$$

where ϵ'_0 , m' , a , and σ_0 are experimental constants. They also made the extremely important assumption that the flexural creep strain, given by

$$\epsilon_F = \frac{y}{\rho}$$

where y is the distance from the neutral axis and ρ the radius of curvature, was identically equal to the tensile creep strain for a corresponding stress. Thus, the ratio of ϵ_T to ϵ_F would be unity, independent of time. The theory of beam deflections which they developed from these assumptions gave good agreement with experimental results only at low stresses, with much less agreement at high stresses.

III. OBJECTIVES OF THE INVESTIGATION

A. Analytical Objective

The objective of the analytical investigation was to describe the form of the curve which results when the ratio of the tensile creep strain to the flexural creep strain for a corresponding stress is plotted against time. If a significant and easily describable curve results, then this curve could be a valuable prediction curve, whereby the flexural creep strain could be predicted for any time from a knowledge of the tensile creep behavior of the material.

B. Experimental Objectives

Specific creep data for alpha uranium in both tension and flexural stress states was sought. It was deemed vital to determine whether or not these creep curves were of the same form, that is, whether the creep rates were the same or proportional for a corresponding stress and the duration of each stage of creep approximately the same. Another important characteristic of the creep curves sought was the nature of the second stage of creep. The ratio of the creep strains was determined and compared with the theoretical values.

Another experimental objective was to observe the change in the creep rate of alpha uranium if, instead of being immediately loaded to a desired stress, the specimen is first

allowed to creep at a lower stress. A stepwise loading should serve to creep harden the material, producing a lower creep rate at any stress than would otherwise be obtained.

IV. THEORETICAL DEVELOPMENT

A. The Creep Stress Distribution in a Beam

The theory of the stress distribution in a beam undergoing flexural creep is of great importance in both the analytical and experimental approaches to the flexural creep problem, and a detailed consideration of this theory is appropriate here.

In determining the stress distribution, the same general development as in the analysis of elastic bending is followed. Five important assumptions are made (12):

1. Bending displacements are small compared with the length of the beam.
2. The plane of bending is a plane of symmetry of the cross section.
3. The analysis is limited to beams that are long compared with their cross-sectional dimensions (approximately ten times), so that deflections resulting from shear can be neglected.
4. Plane sections of the beam before bending remain plane after bending.
5. The stress-strain rate relation for any fiber may be obtained from tensile creep data.

The last two assumptions are of particular importance in predicting the flexural creep behavior of a beam from the

tensile creep data. Assumption four, known as Bernouilli's hypothesis, states that the plastic strains during creep must vary linearly from the neutral axis in order to maintain a plane section. The neutral axis is defined as the line in the stress field where the bending stress is everywhere zero. The validity of Bernouilli's hypothesis is essential in the theoretical determination of the creep stress distribution in a beam. The validity of this hypothesis has been shown experimentally for lead by McCullough and by Tapsell and Johnson. It has also been shown experimentally by Bach (13) for materials which do not obey Hooke's law in both tension and compression. In addition, it has been shown to hold true for alpha uranium (14).

The fifth assumption is the most fundamental to this investigation. Tapsell and Johnson have shown the approximate validity of it for lead beams in flexural creep. A key feature of this assumption is to determine the form of the expression which best describes the variation of tensile stress with creep rate. Finnie and Heller in their book "Creep of Engineering Materials" (12, p. 116) list the four most common groups of empirical expressions which have been used to represent constant stress tensile creep data:

- Constant strain rate
- Time hardening
- Strain hardening
- Recoverable strain included

In the constant strain rate group the strain rate is

assumed to be a function of stress alone. Expressions which have been used to describe this dependence are

$$\begin{aligned}\dot{\epsilon} &= B \sigma^n \\ \dot{\epsilon} &= C e^{\sigma/s} \\ \dot{\epsilon} &= D \sinh \frac{\sigma}{d}\end{aligned}$$

where B, C, D, n, s, and d are experimental constants.

The equation $\dot{\epsilon} = B \sigma^n$ is the one most often found in the literature. Finnie and Heller state that it is adequate "when the steady-state creep contributes most of the strain" and that it is "easiest to use and normally gives a satisfactory fit to the data except perhaps at low stresses." Since this relationship has been shown to hold reasonably well for lead and polystyrene (4, 6), it will also be assumed to be valid for alpha uranium.

In deriving the stress distribution in beams during flexural creep, one begins by considering the two conditions of equilibrium that the beam must satisfy. These are (1):

$$\int_{-c}^c \sigma_y dA = 0 \quad (1)$$

and

$$\int_{-c}^c \sigma_y y dA = M, \text{ the applied moment.} \quad (2)$$

The important assumption is made that the $\dot{\epsilon} = B \sigma^n$ relation obtained from tensile creep tests is applicable to

flexural creep. Thus, the creep rate at a fiber a distance y from the neutral axis is given by

$$\dot{\epsilon}_y = B \sigma^n . \quad (3)$$

Since plane sections are assumed to remain plane,

$$\frac{\epsilon_y}{\epsilon_c} = \frac{y}{c} , \quad (4)$$

where ϵ_c is the strain in the outermost fiber, a distance c from the neutral axis. Thus,

$$\epsilon_y = \epsilon_c \frac{y}{c} .$$

When this expression is differentiated with respect to time, there results

$$\dot{\epsilon}_y = \dot{\epsilon}_c \frac{y}{c} . \quad (5)$$

Equations 3 and 5 are combined to give

$$\frac{\dot{\epsilon}_y}{\dot{\epsilon}_c} = \frac{y}{c} = \frac{B \sigma_y^n}{B \sigma_c^n} .$$

Thus,

$$\sigma_y = \sigma_c \left(\frac{y}{c} \right)^{1/n} . \quad (6)$$

This expression for σ_y is substituted into equation 2 to yield

$$\int_{-c}^c \sigma_c \left(\frac{y}{c} \right)^{1/n} y b dy = M , \quad (7)$$

where $dA = b dy$ for a rectangular cross section ($b \times 2c$).

From the equilibrium condition expressed by equation 1, it can be shown that the neutral axis of the beam coincides with the centroidal axis. Then equation 7 can be written

$$\frac{2 \sigma_c b}{(c)^{1/n}} \int_0^c (y)^{1+\frac{1}{n}} dy = M.$$

When the indicated integration is performed, and use is made of the fact that the moment of inertia I of a rectangular cross section of width b and height $2c$ is $\frac{2}{3} bc^3$, the following stress distribution is obtained:

$$\sigma_y = \frac{Mc}{I} \left(\frac{y}{c}\right)^{1/n} \frac{2n+1}{3n}. \quad (8)$$

Since the term $\frac{Mc}{I}$ is the elastic stress in the outermost fiber of the beam, it is seen that the redistributed stress in this fiber is $\frac{2n+1}{3n}$ of the elastic stress, where n is the slope of the tensile creep rate-tensile stress curve plotted on log paper.

Equation 8 shows how the initial elastic stress distribution in a beam becomes redistributed during creep to a new, steady state stress distribution. This steady state condition is reached when the creep rates in each fiber become proportional to their respective distances from the neutral axis. The time required to achieve this steady state depends on the creep characteristics of the material. For lead this condition is reached twelve minutes after the start of the test (4). Once the steady state is reached, the stress dis-

tribution given by equation 8 remains constant with time.

Equation 8 gives only the steady state stress distribution in a beam. It does not show how the stress distribution varies during transient creep. Goodey (16) and Popov (9) show how the stress distribution varies with time prior to reaching the steady state. Goodey arrives at equation 8 as the limiting case of an integro-differential equation which, when numerically integrated for different values of time, shows how the stress at each fiber varies with time. Goodey's basic assumption was that the stress and creep rate were related by a time hardening law,

$$\dot{\epsilon} = B \sigma^n F(t) ,$$

and not by a constant strain rate relation.

The stress distributions calculated by the methods cited are shown in Fig. 1. Fig. 1(a) shows the steady state stress distribution at $t = t_{\infty}$ as a function of n calculated from equation 8. Three features of the curves are of interest.

1. When $n = 1$, the steady state creep stress distribution is identical to that in the linear elastic case. For $n = 1$, the creep rate is directly proportional to the stress, a situation known as linear viscosity.
2. At large values of n ($n > 20$), the stress distribution is relatively insensitive to changes in n .
3. The initially highly stressed fibers gradually become somewhat relieved of stress, while those fibers

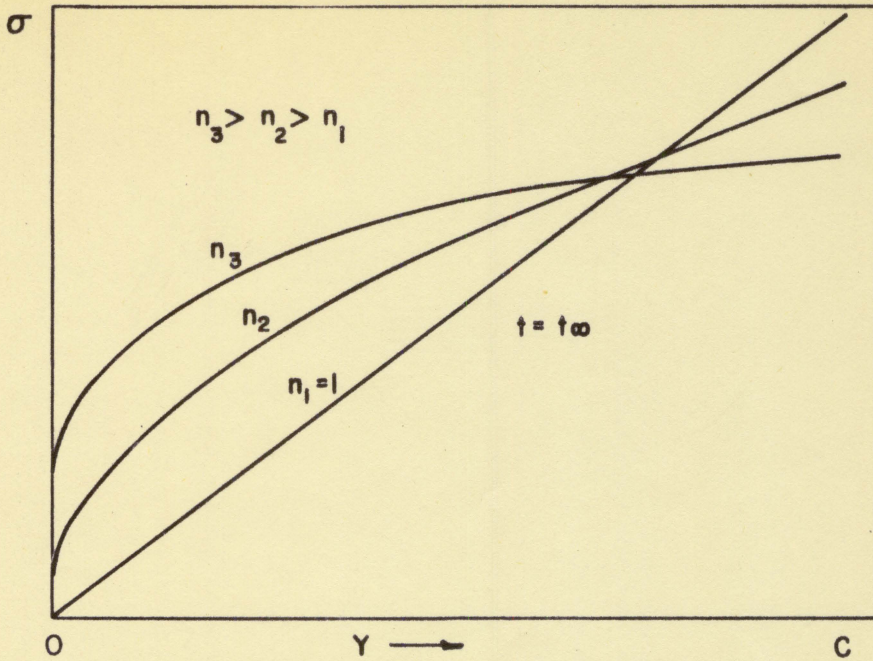


Fig. 1(a). Steady-state stress distribution in a beam by equation 8

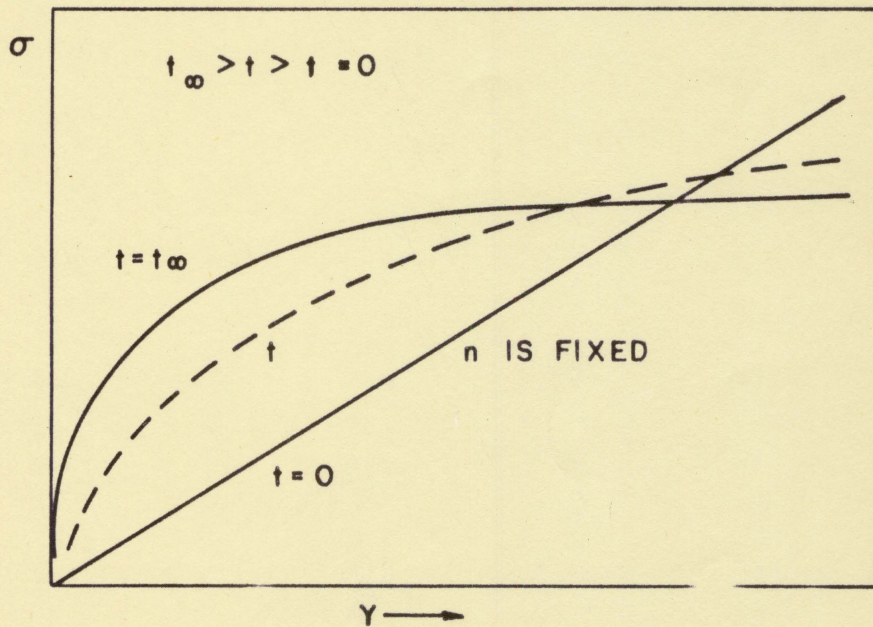


Fig. 1(b). Time-dependent stress distribution in a beam by the method of Goodey

closer to the neutral axis contribute more to the resisting moment.

Fig. 1(b), illustrating the method of Goodey, shows how, for any fixed value of n , the initial elastic stress distribution changes with time until the final steady state distribution, at $t = t_{\infty}$ is reached.

Hoff (17) has pointed out the interesting and useful analogy that exists between creep and non-linear elasticity. Equation 8 may be interpreted as the stress distribution in a beam of material which has a stress-strain curve that follows the non-linear elastic relation $\epsilon = B \sigma^n$.

The practical importance of knowing the redistributed stresses in a beam is that the experimental determination of the creep behavior of a beam must be based upon these stresses and not upon the initial elastic ones.

B. Predicting Flexural Creep Strain from Tensile Creep Strain

No previous investigator has specifically exhibited the relationship between the tensile creep strain and the flexural creep strain at a given stress. However, from the widely made assumption that the creep curves in tension and flexure are of the "same form", it is a simple matter to determine this relationship.

In the following analysis, the subscript T denotes tension and F flexure. If $\dot{\epsilon}_T = B \sigma^n$ expresses the minimum,

second stage creep rate in tension as a function of the stress, then the minimum, second stage creep rate in flexure is assumed to also be given by

$$\dot{\epsilon}_F = \dot{\epsilon}_T = B\sigma^n \quad (9)$$

Since this expression relates stress to the second stage (constant) creep rate and ignores the transient creep period, it is possible for these first stage creep rates to be different. This possibility could account for what differences in the mechanisms of creep may exist under both types of stress states. Thus the creep curves need not necessarily be identical, and in the most general case would look like

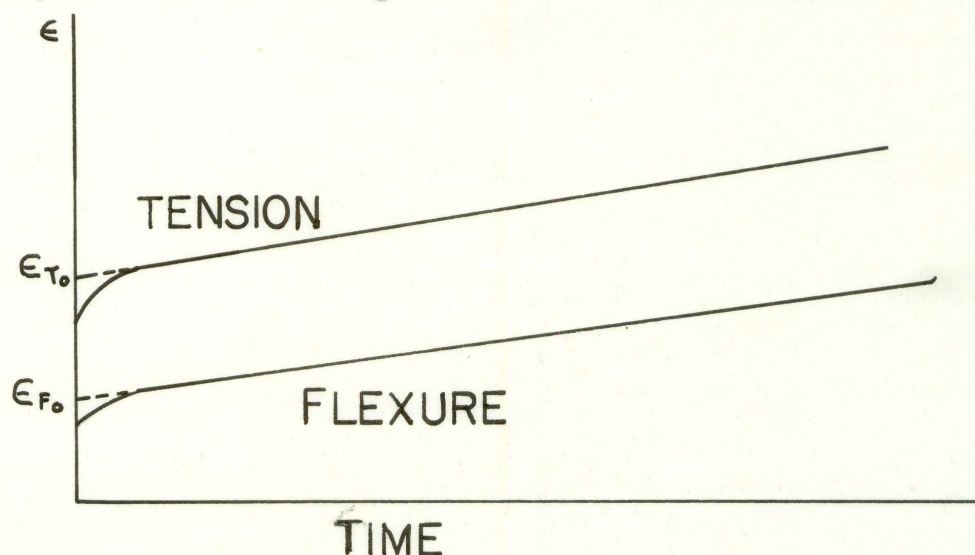


Fig. 2. Tensile and flexural creep curves having the same form

If it is assumed that the first stage of creep is short enough so that the creep curve is essentially composed of a linear region, the curves may be represented by equations of

the form

$$\begin{aligned}\epsilon_T &= \dot{\epsilon}_T t + \epsilon_{T_0} \\ \epsilon_F &= \dot{\epsilon}_F t + \epsilon_{F_0}\end{aligned}\quad (10)$$

where ϵ_{T_0} and ϵ_{F_0} are the values of the tensile and flexural creep strains obtained by extrapolating the linear portions of the creep curves back to $t = 0$.

Now, since $\dot{\epsilon}_F = \dot{\epsilon}_T$,

$$\begin{aligned}\frac{\epsilon_T - \epsilon_{T_0}}{t} &= \frac{\epsilon_F - \epsilon_{F_0}}{t} \\ \epsilon_T - \epsilon_F &= \epsilon_{T_0} - \epsilon_{F_0} \\ \frac{\epsilon_T}{\epsilon_F} - 1 &= \frac{\epsilon_{T_0} - \epsilon_{F_0}}{\epsilon_F} \\ \frac{\epsilon_T}{\epsilon_F} &= 1 + \frac{(\epsilon_{T_0} - \epsilon_{F_0})}{\epsilon_F} \\ \frac{\epsilon_T}{\epsilon_F} &= 1 + \frac{\epsilon_{T_0} - \epsilon_{F_0}}{\dot{\epsilon}_T t + \epsilon_{F_0}}.\end{aligned}\quad (11)$$

Thus, the ratio of tensile creep strain to flexural creep strain varies inversely with time. Of course, if the creep curves are identical so that $\epsilon_{T_0} = \epsilon_{F_0}$, then $\epsilon_T = \epsilon_F$ and the tensile creep strain is identical to the flexural creep strain. The degree by which $\epsilon_{T_0} - \epsilon_{F_0} > 0$ determines the rate of change of $\frac{\epsilon_T}{\epsilon_F}$ with time.

The important assumption that the minimum creep rates are the same seems to be altogether too restrictive. It is logical to suppose that, when a bending moment subjects a beam to an extremely steep stress gradient along its cross section, the creep in each fiber depends in some way upon the interaction of this fiber with adjacent fibers. If this interaction is complex, then the form of the flexural creep curve may be radically altered from that of the tensile creep curve. If the forms of the curves are not the same, then it is possible for one curve to be in transient creep in the same time interval that the other curve is in second stage creep, and it is also possible that the minimum creep rates might never be equal.

Let the creep rates in tensile and flexural creep now be expressed by

$$\begin{aligned}\dot{\epsilon}_T &= B_T \sigma^{n_T} \\ \dot{\epsilon}_F &= B_F \sigma^{n_F} .\end{aligned}\quad (12)$$

Again, it is assumed that the creep curves can be represented by equations of the form

$$\begin{aligned}\epsilon_T &= \dot{\epsilon}_T t + \epsilon_{T_0} \\ \epsilon_F &= \dot{\epsilon}_F t + \epsilon_{F_0}\end{aligned}$$

where ϵ_{T_0} and ϵ_{F_0} are defined as before. Thus,

$$\frac{\dot{\epsilon}_T}{\dot{\epsilon}_F} = \frac{\epsilon_T - \epsilon_{T_0}}{\epsilon_F - \epsilon_{F_0}} = \frac{B_T}{B_F} \sigma^{n_T - n_F} = K$$

$$\epsilon_T - \epsilon_{T_0} = K(\epsilon_F - \epsilon_{F_0})$$

$$\epsilon_T - K\epsilon_F = \epsilon_{T_0} - K\epsilon_{F_0}$$

$$\frac{\epsilon_T}{\epsilon_F} - K = \frac{\epsilon_{T_0} - K\epsilon_{F_0}}{\epsilon_F}$$

$$\frac{\epsilon_T}{\epsilon_F} = K + \frac{\epsilon_{T_0} - K\epsilon_{F_0}}{\dot{\epsilon}_F t + \epsilon_{F_0}} \quad (13)$$

Therefore, the ratio $\frac{\epsilon_T}{\epsilon_F}$ again varies inversely with time.

A comparison of equations 13 and 11 shows that when the creep rates are the same the flexural creep strain can be predicted much more directly from tensile creep data than when the creep rates are not the same. In the first case, the only flexural creep parameter which need be known for the prediction is ϵ_{F_0} which in many cases may be approximately deduced. In the latter case, not only must ϵ_{F_0} be known, but also the flexural creep rate and the constant $K = \frac{B_T}{B_F} \sigma^{n_T - n_F}$.

A most important point has been raised from the preceding discussion. Since it is possible that n_T does not equal n_F for the case of dissimilar creep rates in tension and flexure, is the stress distribution in the beam as calculated from equation 8 (which was derived assuming that n_T and n_F are

equal) correct? Although the stress distribution is now not exactly correct, the insensitivity of the stress distribution to changes in n when n is large renders equation 8 a most acceptable approximation to the actual stress distribution for plastic and semi-plastic materials, which have large values of n .

Another means of obtaining the ratio $\frac{\epsilon_T}{\epsilon_F}$ is by the selection of a mathematical model for creep. Pao and Marin (10) give the most general expression for a creep curve under constant stress as

$$\epsilon = \frac{\sigma}{E} + K \sigma^a (1 - e^{-qt}) + B \sigma^\beta t, \quad (14)$$

where the first term on the right hand side represents the initial elongation, the second term the first stage region, and the third term the second stage (linear) region of the creep curve. This equation is of the form

$$\epsilon = C + D(1 - e^{-qt}) + Gt, \quad (15)$$

where C , D , q , and G are experimental constants. Then, the most general form of the ratio of the tensile creep strain to the flexural creep strain is

$$R(t) = \frac{\epsilon_T(t)}{\epsilon_F(t)} = \frac{C_T + D_T(1 - e^{-q_T t}) + G_T t}{C_F + D_F(1 - e^{-q_F t}) + G_F t} \quad (16)$$

which is the ratio of two trinomials. Information concerning the relative magnitudes of $\frac{D_T}{D_F}$, $\frac{q_T}{q_F}$ and $\frac{G_T}{G_F}$ is needed before

this expression can be further manipulated. This information will be obtained experimentally. If, as in the cases of lead and polystyrene, the term $C + D(1 - e^{-qt})$ can be replaced by a constant, and $G_T = \dot{\epsilon}_T = G_F = \dot{\epsilon}_F$, then equation 16 reduces to equation 11.

V. PROCEDURE

A. General Procedure

Eight tensile creep tests were run at stresses ranging from 78,450 psi to 90,450 psi. The linear creep rates were determined for four of these stresses (78,450, 82,450, 86,450, and 88,450 psi). Two of the specimens, at stresses of 88,450 and 90,450 psi fractured immediately upon loading, and the remaining two were used in the determination of the creep hardening phenomenon in alpha uranium.

A log plot of the stress-creep rate data confirmed the fact that the power law relation is a valid one for alpha uranium. The value of n was obtained by a least squares fit. The values of the linear creep rates were also determined by a least squares analysis of the creep curves. The value of n thus obtained was used to calculate the stress distribution in the beam by means of equation 8. SR-4 strain gages were then cemented to those fibers of the beam at which the calculated value of the flexural stress was numerically equal to the tensile stress for which tensile creep data had been obtained. In this way, it was possible to make a direct comparison between the tensile and flexural creep strains for corresponding values of stress and time.

B. Tensile Creep Tests

1. Material

The material used in this investigation was extruded beta quenched natural uranium which was supplied in four-inch slugs 1.375 inches in diameter. This material is described by the supplier as having less than 0.1 per cent of the impurities C, Cl, Cr, Si, B, Mg, Ni, and N.

Lewis (18) gives room temperature tensile properties for nine specimens of this material, from which the following data were obtained:

Modulus of elasticity (average value for six tension cycles):	21,800,000 psi
Yield strength at 0.1 per cent offset:	33,500 psi
Ultimate strength:	91,200 psi
Reduction of area:	9 per cent
Elongation in 1 inch:	8 per cent

The material has an endurance limit in rotating bending (500,000,000 revolutions) of about 25,000 psi at 50°C.

The alpha phase of uranium is stable at temperatures less than 660°C and has an orthorhombic crystalline structure. The non-symmetric structure of uranium single crystals causes anisotropic strength properties which are reflected on polycrystalline specimens because a certain amount of preferred orientation occurs during the forming and heat treatment. Uranium is not an ideal material for experimentation purposes

due to the lack of high correlation between theoretical predictions and experimental results (19), and to the non-reproducible nature of much data (20). An example of this latter characteristic was experimentally obtained in this study. One tensile creep specimen stressed to 86,450 psi crept for over three hours with a well defined linear creep region, while another specimen at this same stress fractured immediately upon loading.

Specimens were fabricated by quartering the slug longitudinally and turning. The length of the specimen was four inches and each end was 0.500 inch in diameter. The ends were threaded 0.75 inch with a 1/2-13NC thread. The reduced section in the center was 0.357 inch in diameter (cross sectional area 0.100 square inch) and two inches long. Into the unthreaded part of the shoulder at each end two gage holes were drilled diametrically opposite with the pair at one end 90° from the pair at the other end. The longitudinal distance between holes at opposite ends was 2.25 inches. The holes were drilled 0.125 inch deep with a number 38 drill. Accurate positioning of the holes was accomplished by means of a drill jig supplied with the creep machine. The dimensions of this specimen agree with those recommended by the A.S.T.M. (21) for creep tests.

2. Apparatus

A 12,000 pound capacity Baldwin lever arm creep machine was used in the test. The calibration reports on this machine showed the machine loading error to be approximately 0.1 per cent in the range of loads used. The machine was equipped with an extensometer of the electrical motor-contact follower type connected to a counter. Each division of the counter was equivalent to a specimen elongation of 25 micro-inches. The machine was also equipped with a clock motor-driven time counter with each division equivalent to one-tenth hour. A galvanized hood was mounted on the machine to protect the specimens from air convection currents which cause irregular thermal fluctuations, disturbing the consistency of the strain measurements. The hood had a plexiglass window, through which the clock readings and the readings of a thermometer mounted near the specimen were read. Further insulation was obtained by using pyrex wool and a covering of transite above and below the hood.

C. Flexural Creep Tests

1. Material

A rectangular bar, $1/2$ in. by 1 in. by $8\ 3/8$ in. was milled from a slug of alpha uranium 1.375 in. in diameter and $8\ 3/8$ in. long. The longitudinal centroidal axis of the bar

was made to correspond to that of the slug to maintain the symmetry of the state of the crystal structure.

2. Apparatus

A special rigid steel frame was built in order to adapt the Baldwin lever arm creep machine for flexure tests. A diagram of the frame with the bar specimen in the test position is shown in Fig. 3.

The reaction of the lever arm to the applied load is transmitted to the flexure specimen through rollers, which approximate a point contact. The reaction forces on the specimen act through knife edges fastened to the top plate of the frame. These knife edges also approximate a point contact. With the rollers transmitting the load, and the knife edges the reaction forces, and both rollers and knife edges in fixed positions, a section of constant moment on the specimen is maintained. This section of constant moments exists between the rollers.

SR-4 strain gages were cemented to the appropriate positions on the face of the beam. Each position was located to within 0.001 in. by means of a carefully calibrated L. S. Starret gage. Gages were positioned at fibers corresponding to flexural stresses of +86,450 psi, -86,450 psi, +78,450 psi, +82,450 psi, +84,017 psi, and -84,017 psi, where the + sign refers to the tensile side of the neutral axis and the - sign

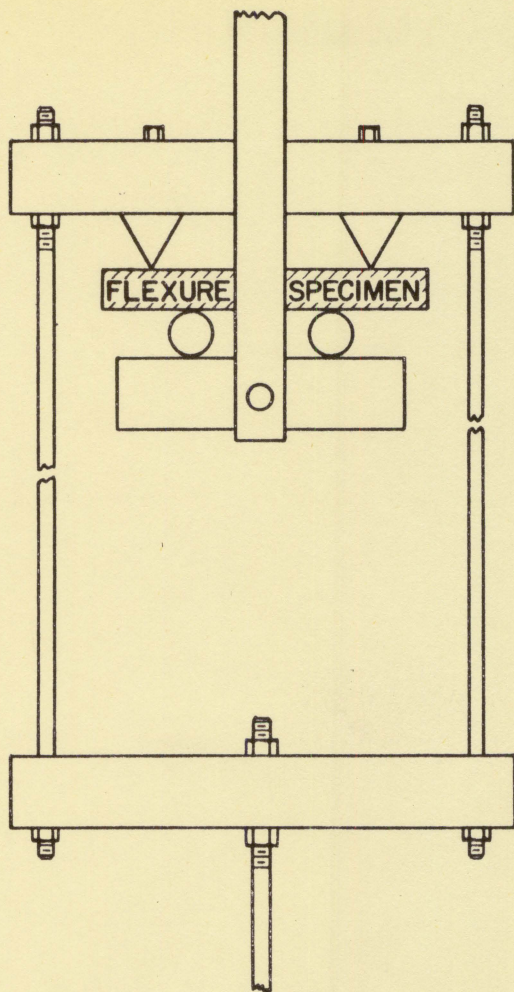


Fig. 3(a). Frame used in flexure tests

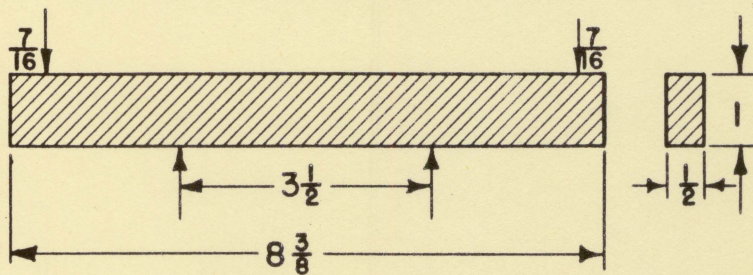


Fig. 3(b). Loading scheme of the bar specimen of alpha uranium

to the compressive side. The stress distribution calculated from equation 8 was designed to produce stresses of $\pm 86,450$ psi in the extreme fibers of the beam. All of the stresses except $\pm 84,017$ psi were designed to correspond directly to those employed in the tensile creep tests. The stresses $\pm 84,017$ psi were the stresses which corresponded to two gage positions arbitrarily selected to record the ratio of the creep strain on the tensile side of the neutral axis with that on the compressive side.

The flexural creep strains at each gage position were measured directly by an SR-4 Strain Indicator. Number 20 single strand wire leads were soldered to the terminals of the strain gages and connected to the terminals of a Baldwin-Hamilton 20 Point Switching Unit, which in turn was connected to the Strain Indicator. Thus, by simply switching to different terminals of the Switching Unit, the strain at any desired strain gage could be directly read at any time.

In accordance with standard SR-4 strain gage procedure (22), a strain gage mounted on a small piece of uranium was placed in close proximity to the specimen and connected to the Switching Unit. Thus, satisfactory temperature compensation was attained.

The galvanized hood and insulations mentioned previously helped keep the thermal fluctuations to a minimum.

It cannot be too strongly emphasized that great care must

be exerted in positioning the strain gages on the beam accurately. The distance from the neutral axis of the beam to the outermost fiber (where the stress was 86,450 psi) was 1/2 in. Yet the stress at just 0.0055 in. away from the neutral axis was 78,450 psi. With this exceedingly steep stress gradient, it is easy to envision how a slight error in positioning the gage could produce a noticeable error in the stress. For example, if the gage were positioned with an error of just 0.0005 in., so that the actual position of the gage 0.0060 in. from the neutral axis, the actual stress would be 78,589 psi. The steep stress gradient present in the vicinity of the neutral axis levels off and is very gentle over most of the beam face.

VI. EXPERIMENTAL RESULTS

Figs. 4-7 show the room temperature tensile creep curves of alpha uranium at the four stresses employed in the tests. The strain readings were not recorded automatically, and in each case no third stage creep data or exact time to failure were recorded. The values of the minimum strain rates obtained from the second stage creep data are given in Table 1.

Table 1. Minimum tensile creep rates for alpha uranium at room temperature

Stress psi	Creep rate min ⁻¹
78,450	8.616×10^{-7}
82,450	2.869×10^{-6}
86,450	4.552×10^{-5}
88,450	1.653×10^{-4}

Fig. 8 shows the power law relation between creep rate and stress. By a least squares analysis, a value of $n = 46.39$ was obtained and was used in determining the stress distribution in the beam. Creep data for the outermost fiber at a stress of $-86,450$ psi was not obtained, since the strain in this fiber immediately exceeded the 40,000 micro-inch per inch limit of the Strain Indicator.

Figs. 9-12 show the room temperature flexural creep curves of the bar specimen of alpha uranium.

Figs. 13, 14 and 15 show the ratio of the tensile creep strain to the flexural creep strain at three stresses plotted against time. For some of the points, both ϵ_T and ϵ_F were measured directly at a given time. At other points, a corresponding reading of one of the strains was not obtained at a certain time, and the value of this strain at the time in question was obtained from the appropriate creep curve.

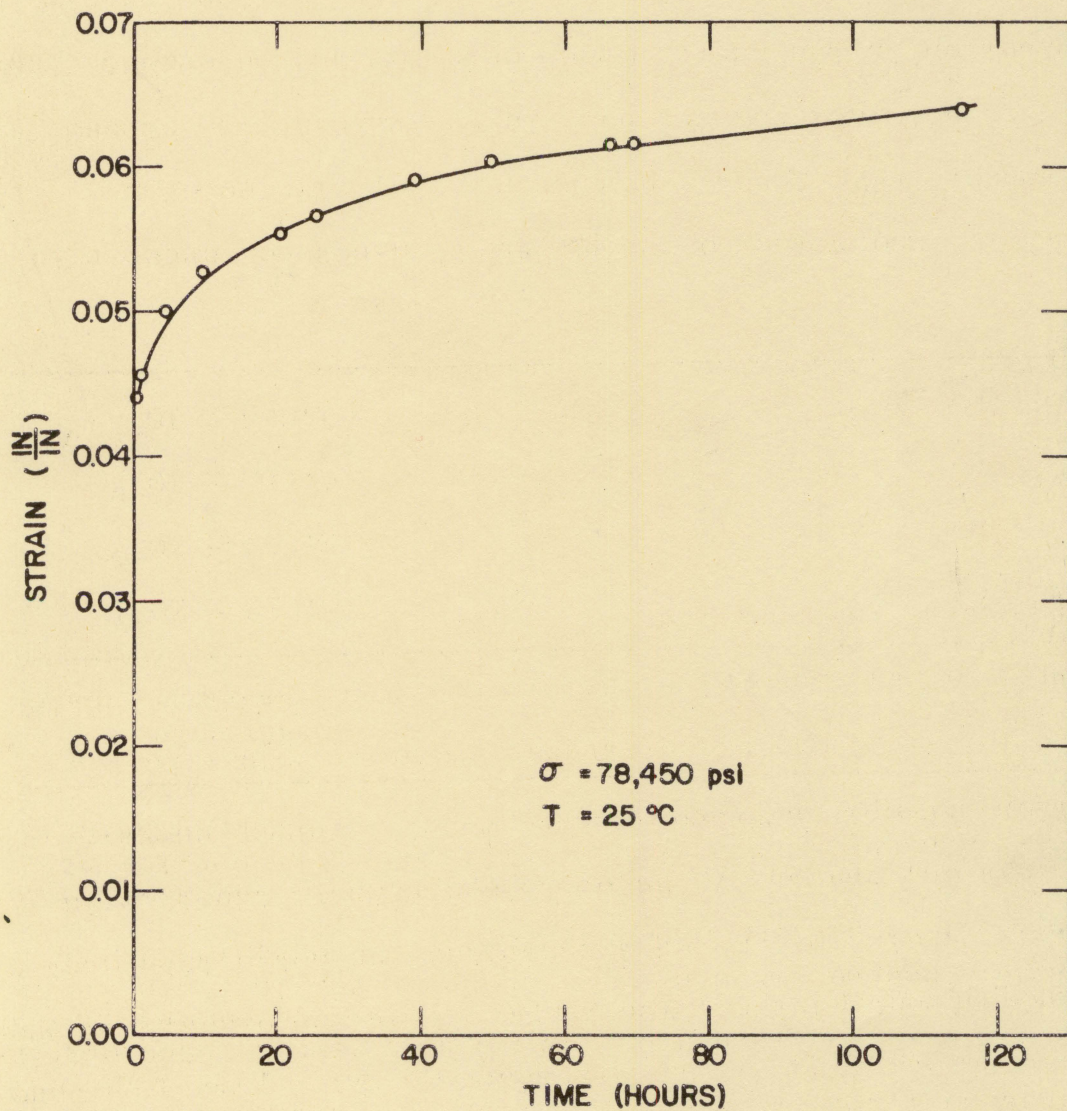


Fig. 4. Tensile creep curve at $\sigma = 78,450 \text{ psi}$

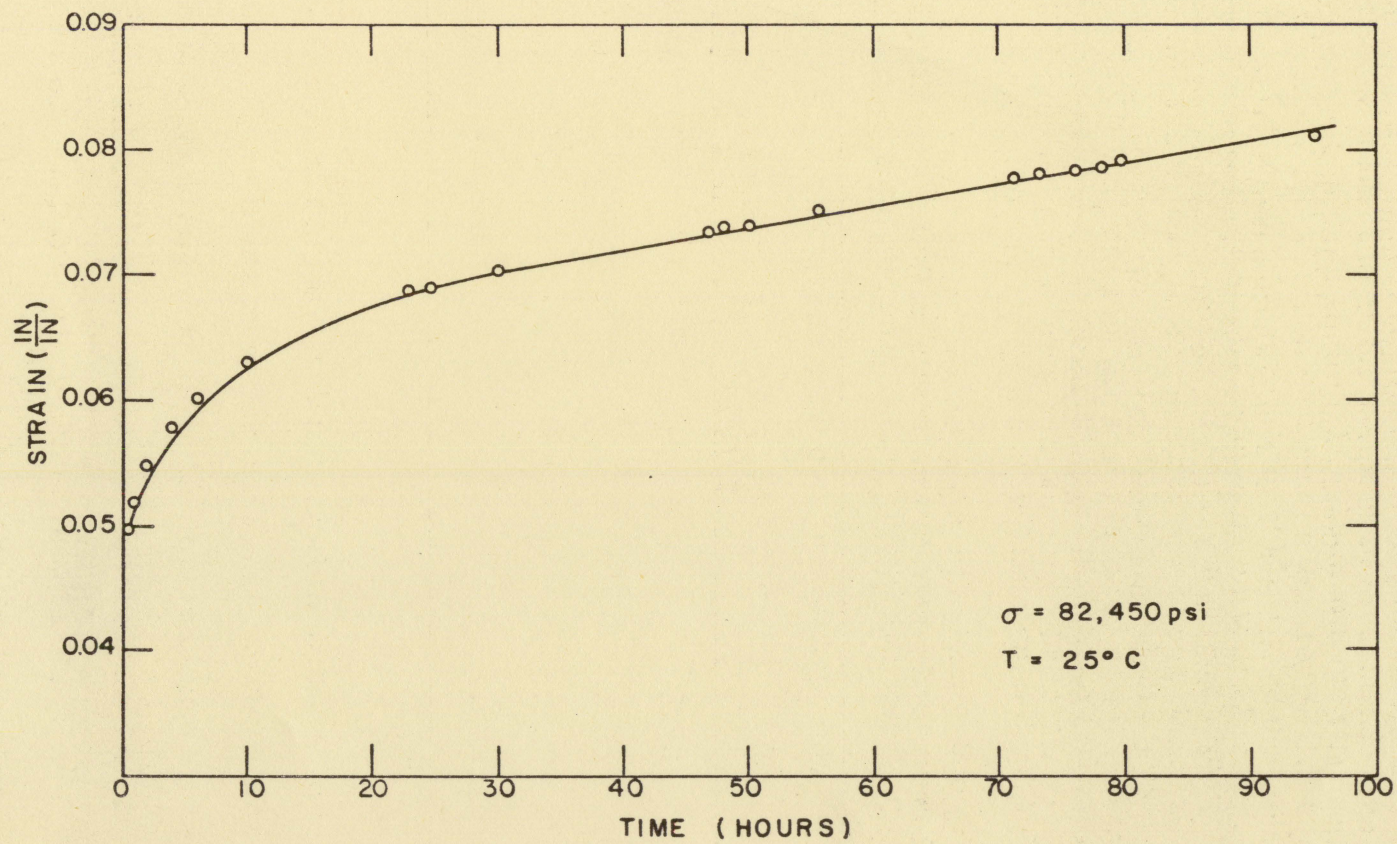


Fig. 5. Tensile creep curve, $\sigma = 82,450$ psi

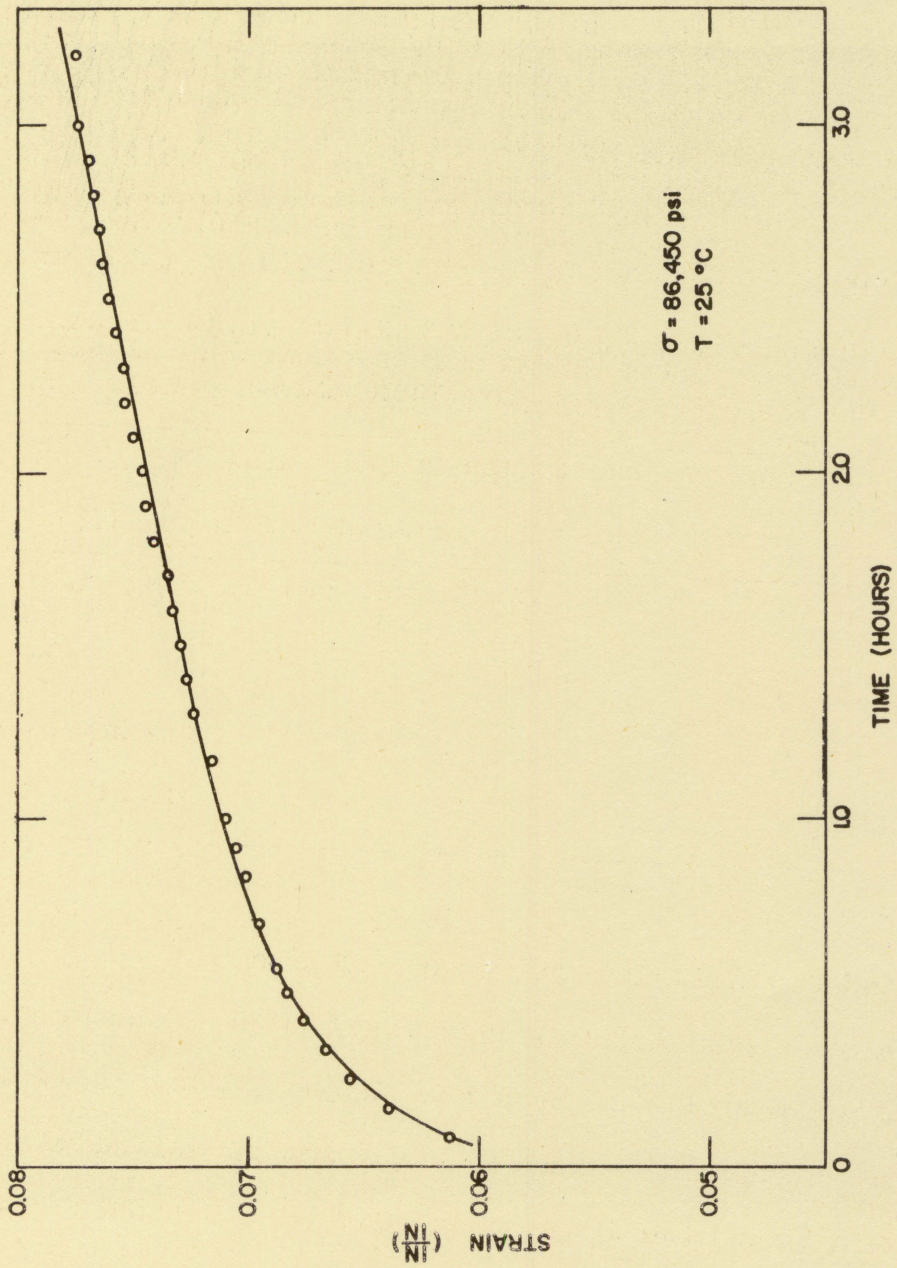


Fig. 6. Tensile creep curve, $\sigma = 86,450$ psi

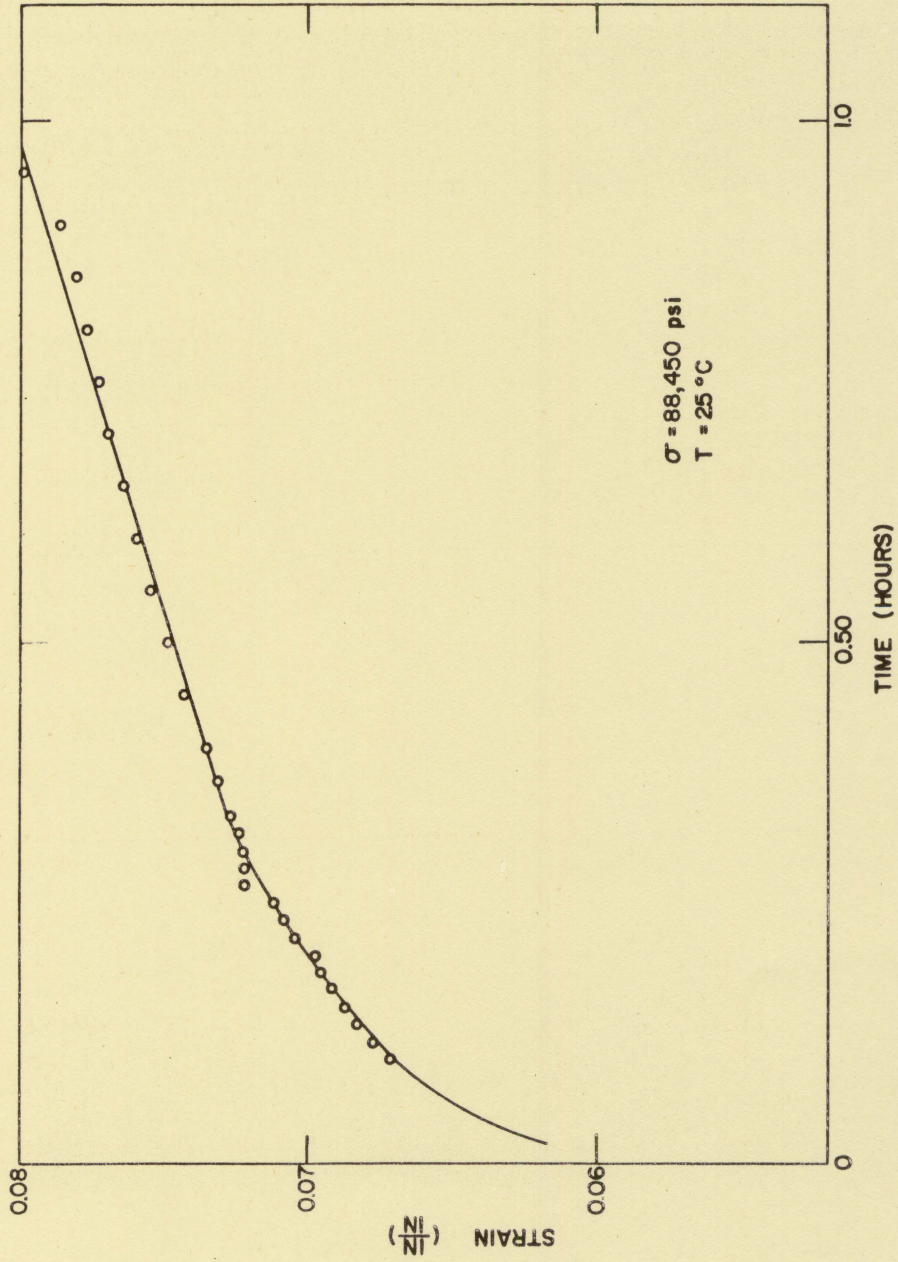


FIG. 7. Tensile creep curve, $\sigma = 88,450 \text{ psi}$

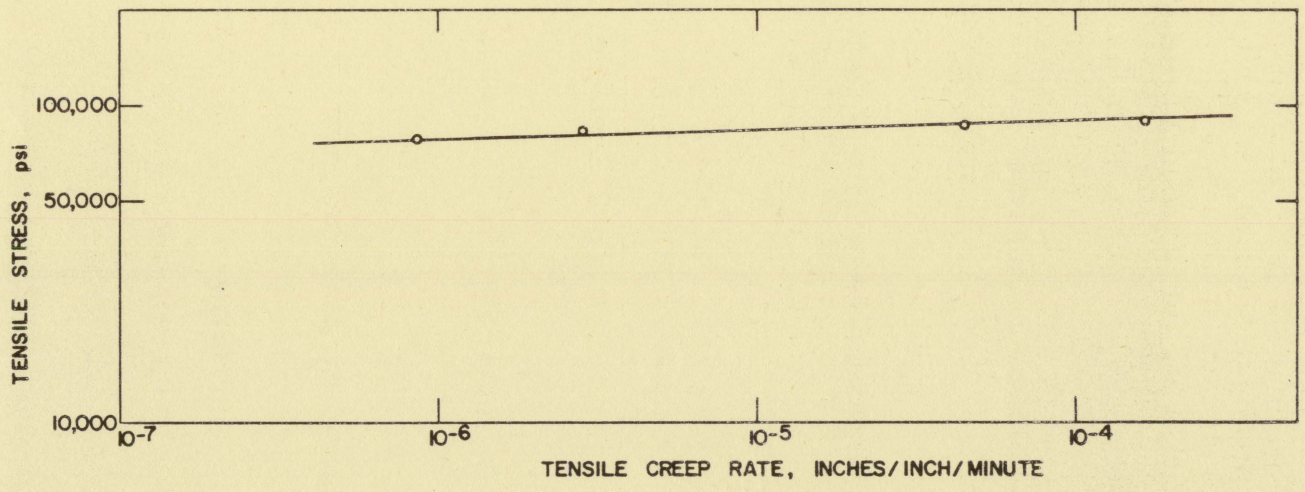


Fig. 8. The power law relation between stress and creep rate

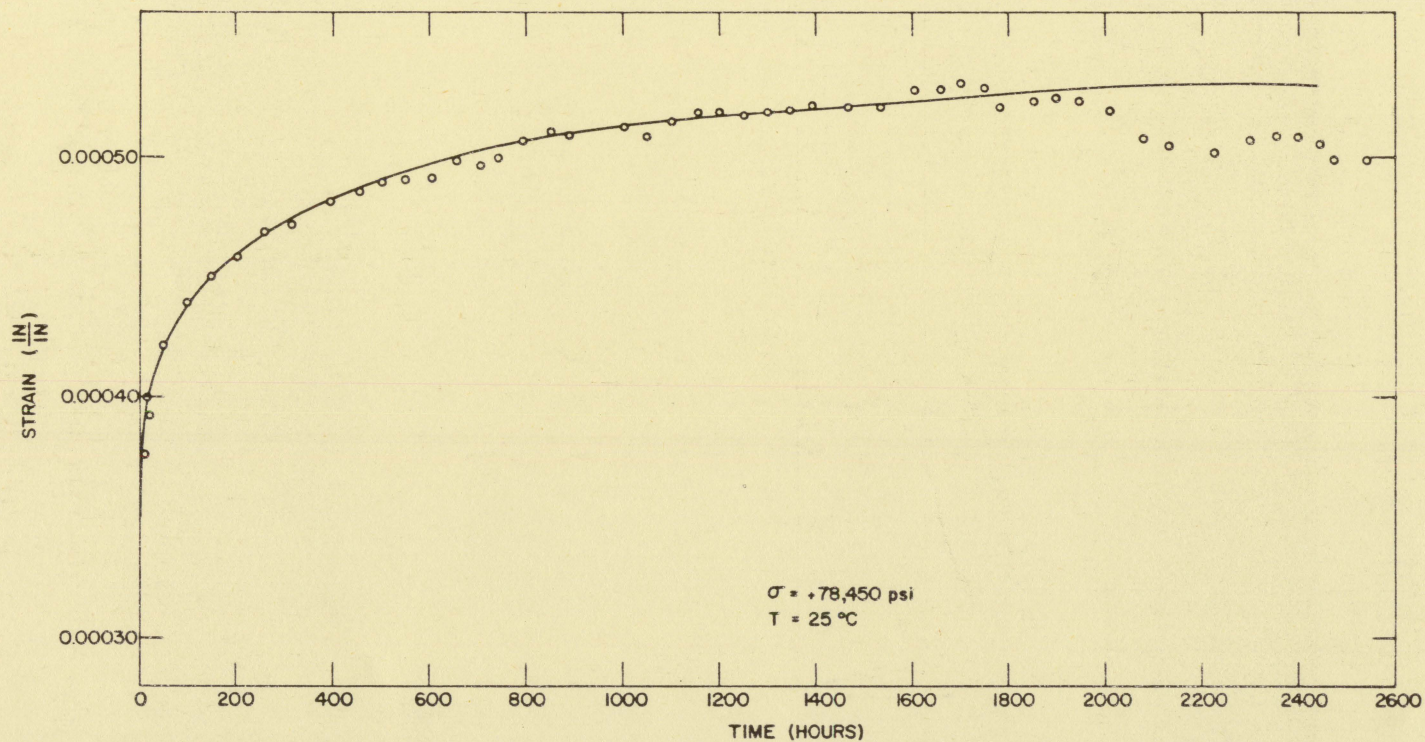


Fig. 9. Flexural creep curve at $\sigma = +78,450 \text{ psi}$

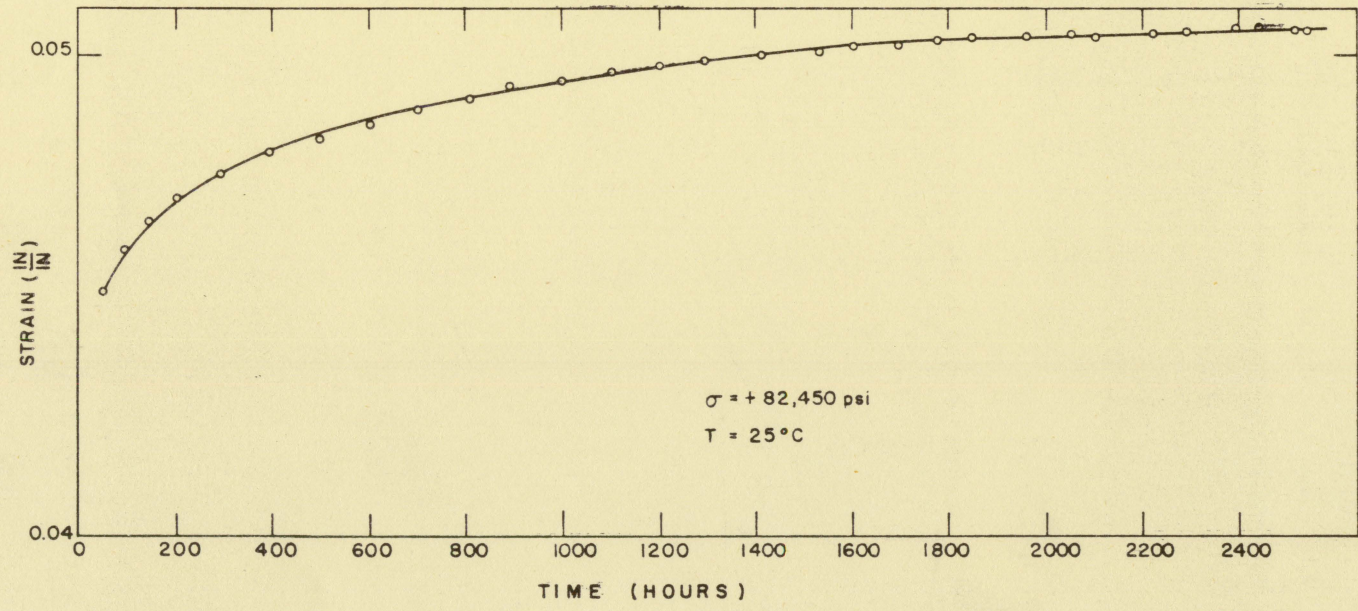


Fig. 10. Flexural creep curve at $\sigma = +82,450$ psi

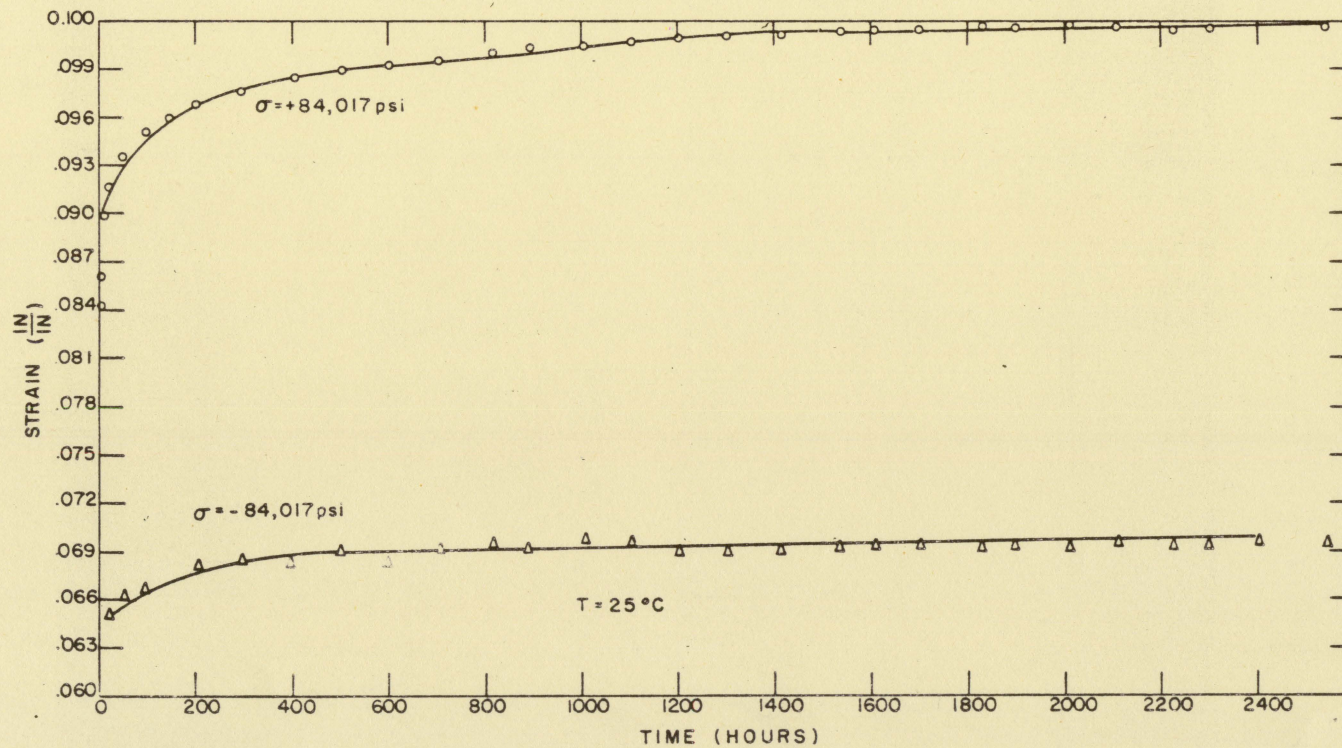


Fig. 11. Flexural creep curves at $\sigma = +84,017 \text{ psi}$ and $\sigma = -84,017 \text{ psi}$

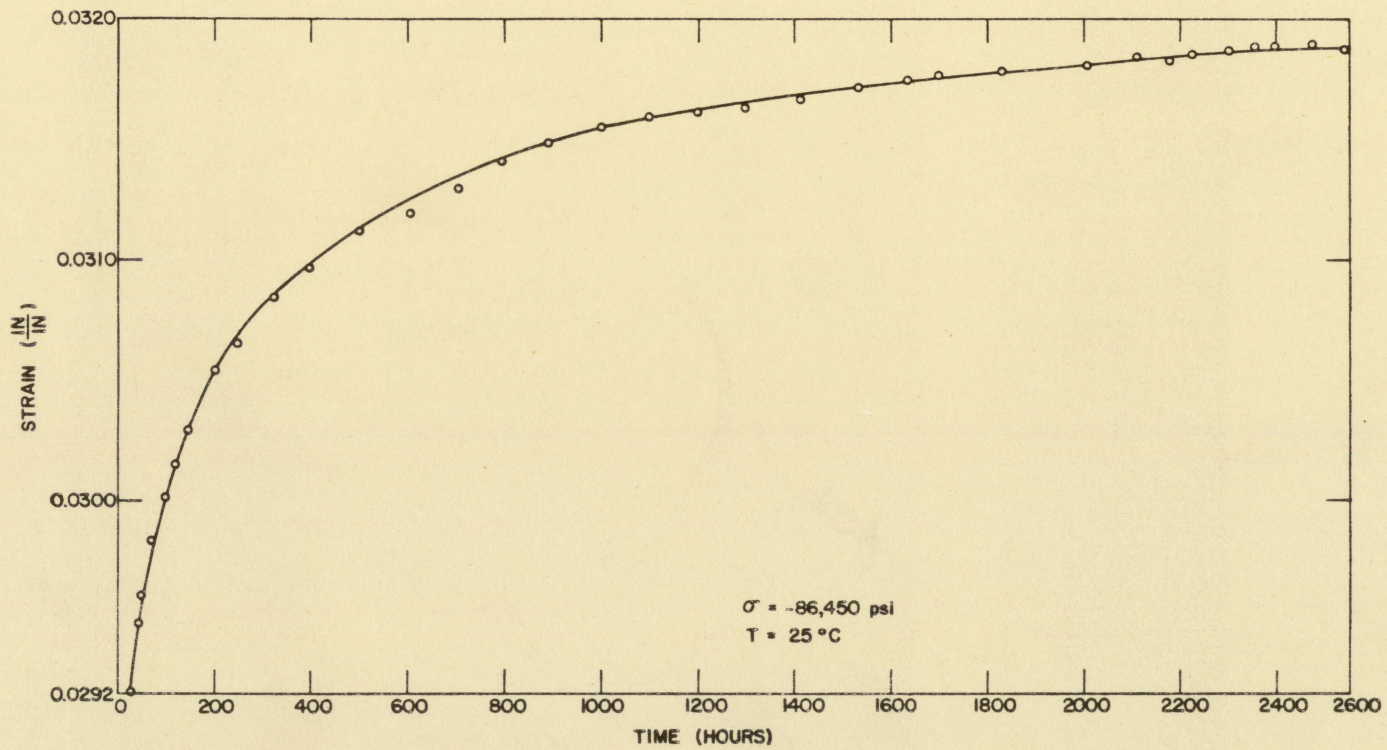


Fig. 12. Flexural creep curve at $\sigma = -86,450$ psi

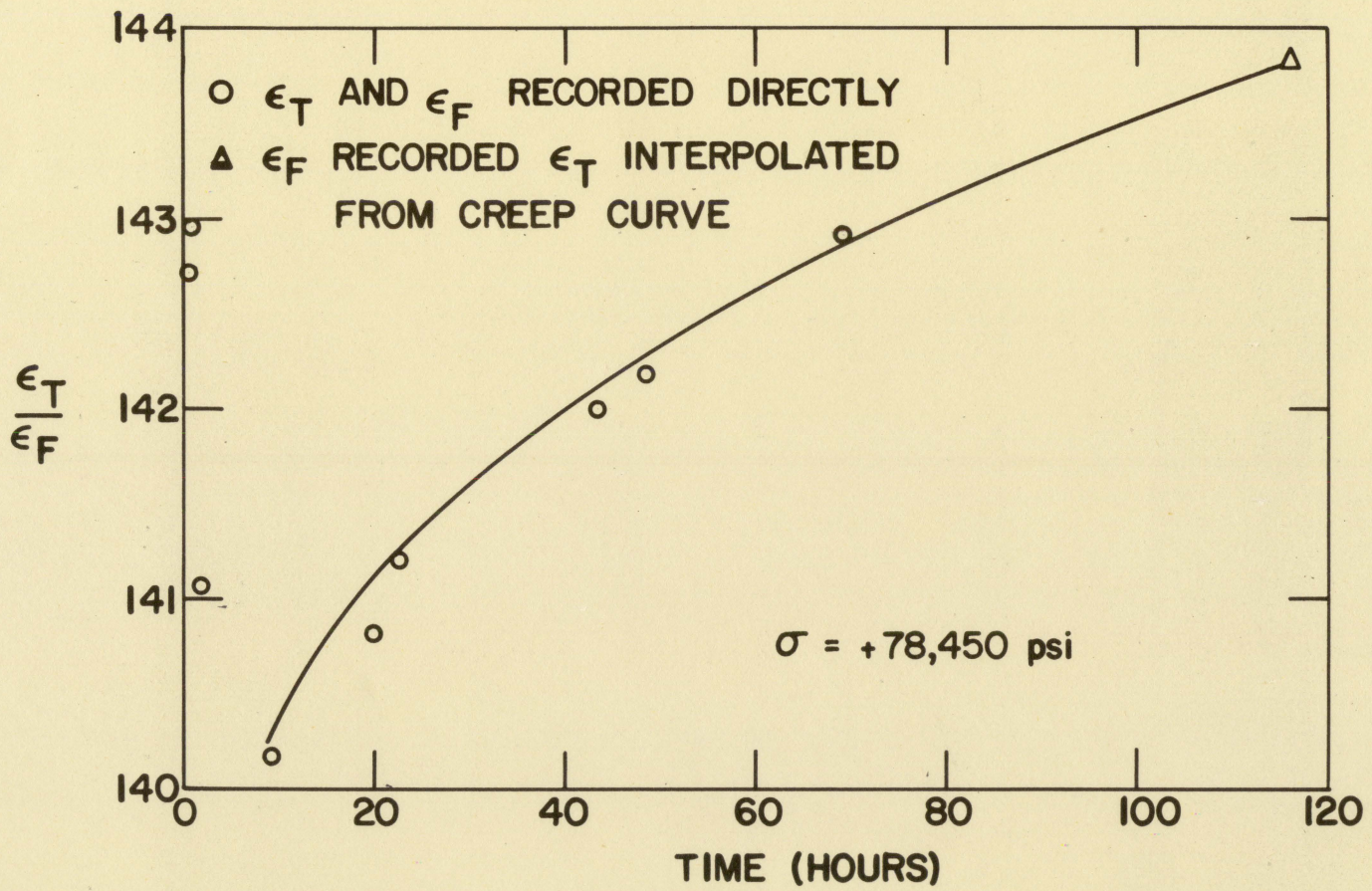


Fig. 13. Ratio curve at $\sigma = 78,450 \text{ psi}$

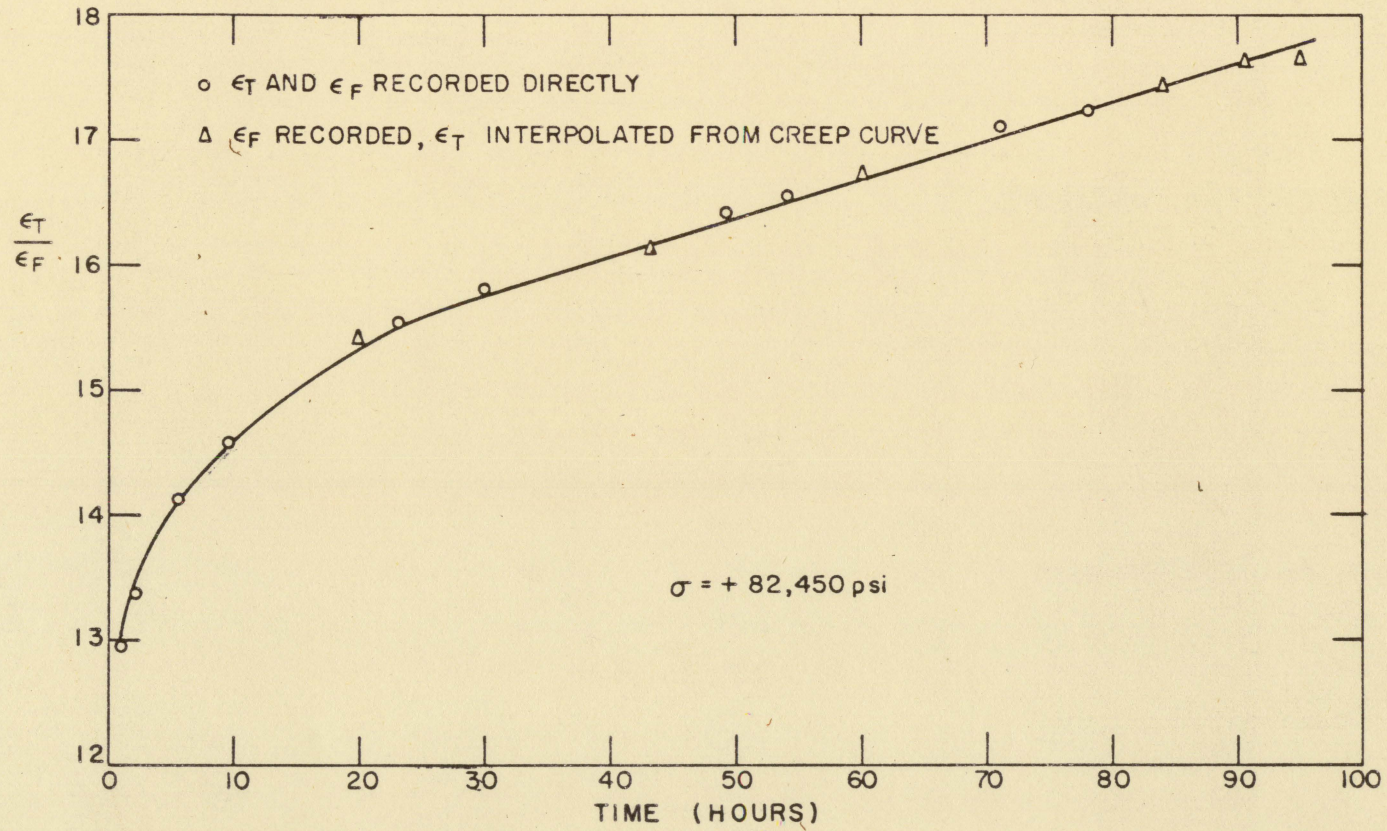


Fig. 14. Ratio curve at $\sigma = 82,450$ psi

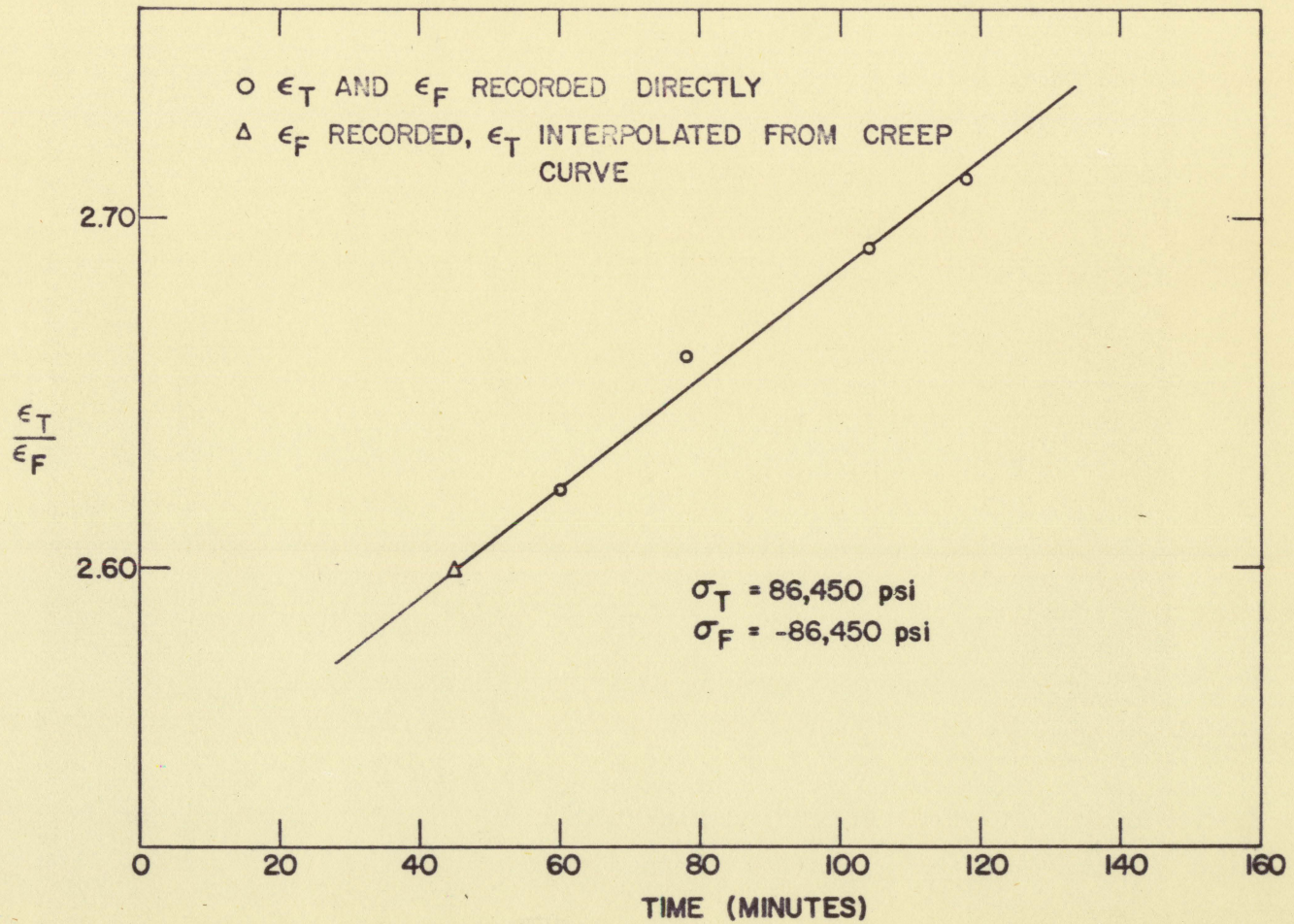


Fig. 15. Ratio curve at $\sigma = 86,450$ psi

VII. DISCUSSION OF RESULTS

A. The Creep Curves

In comparing the tensile and flexural creep curves for the two stresses where a direct correlation can be made (+78,450 and +82,450 psi), as well as the stress at which an approximate comparison can be made (86,450 psi), a striking result stands out. The creep curves do not have the same characteristics. Five important differences are apparent:

1. The duration of the transient period of creep is much longer in flexural creep than in tensile creep.
2. The second stage period of creep is also much longer in flexural creep.
3. The tensile creep curves show a well defined linear range. The flexural creep curves do not.
4. The magnitude of the tensile creep strain is greater than that of the flexural creep strain at corresponding stresses and times.
5. The second stage flexural creep rates are much smaller than the second stage tensile creep rates at corresponding stresses.

Some elaboration will now be given on each of these important differences. Consideration will first be given to the transient creep behavior of the creep curves. At a stress of 82,450 psi, for example, the first stage portion of the

tensile creep curve endures for 27 hours. The first stage region of the flexural creep curve at this stress endures for about 1000 hours. At a stress of 78,450 the times of first stage creep are 50 hours and about 1000 hours, and at 86,450 psi the times are $1 \frac{1}{3}$ and 1000 hours.

A consideration of second stage creep at 82,450 psi reveals that the tensile creep curve exhibits a time region of about 80 hours prior to failure. The flexural creep tests were terminated after over 2500 hours of testing. About 1500 hours of this total may be considered to constitute the second stage region, and at the conclusion of the tests no evidence of impending fracture was apparent. The term "second stage" creep is used advisedly in referring to the flexural creep behavior, for, as the third difference cited above states, the flexural creep curves do not show the well defined second stage (linear) region that the tensile creep curves do. The flexural creep rates continually decrease with time for each of the stresses at which creep strains were recorded. Thus, at any stress, the tensile creep specimen has gone through the three stages of creep to failure, while a beam fiber in flexural creep is still exhibiting a long first stage region. This result has not been previously reported, and will certainly affect an important change in the prediction formulae, equations 11 and 13.

Not only are the magnitudes of the tensile creep strains

greater than those of the flexural creep strains, but the strain rates are also larger. Since the second stage regions of the flexural creep curves exhibit a continually decreasing creep rate, it is not possible to refer to a linear creep rate which defines these curves over the entire second stage. However, close analysis of the curves shows that, for certain time intervals, it is possible to determine a linear creep rate which closely approximates the true creep rate over that time interval. The time intervals of 200-330 hours, 500-900 hours, and 1000 to 1600 hours can be analyzed in this manner. Flexural creep rates were determined for these intervals by a least squares fit to the data. Then a value of n was obtained for the interval assuming the power law between creep rate and stress. These values of n were compared with the value of n obtained from the tensile tests. This information is given in Table 2.

To summarize, the tensile and flexural creep curves for alpha uranium at room temperature are definitely not of the same form. The fact that the exponent n varies with time indicates that the relation $\dot{\epsilon}_F = B\sigma^n$ is not strictly valid since $\dot{\epsilon}_F$ is not the minimum creep rate. Also, n_T will never equal n_F , since the continually decreasing flexural creep rates continually show a greater deviation from the minimum tensile creep rates.

Excessive scatter in the flexural creep data at a stress

Table 2. Comparison of the creep rates and the exponent n for tensile and flexural creep of alpha uranium

σ psi	$\dot{\epsilon}_T$ min ⁻¹	$\dot{\epsilon}_F$ min ⁻¹ 200-330 hours	$\dot{\epsilon}_F$ min ⁻¹ 500-900 hours	$\dot{\epsilon}_F$ min ⁻¹ 1000-1600 hours
78,450	8.616×10^{-7}	1.707×10^{-8}	8.042×10^{-10}	4.222×10^{-10}
82,450	2.869×10^{-6}	6.287×10^{-8}	4.542×10^{-9}	1.972×10^{-9}
84,017	--	6.207×10^{-8}	5.917×10^{-9}	2.433×10^{-9}
86,450	4.552×10^{-5}	5.258×10^{-7}	2.895×10^{-8}	1.653×10^{-8}
88,450	1.653×10^{-5}	--	--	--
n	46.39	36.36	36.45	38.10
% diff. in n	0	21.56	21.43	17.87

of +78,450 psi after 1800 hours of testing indicates failure of the strain gage.

It was found that the creep strain at +84,017 psi was about 1 1/2 times as large as that at $\sigma = -84,017$ psi. If it is assumed that this ratio holds for every fiber on both sides of the neutral surface, then the creep curve at $\sigma = +86,450$ psi can be approximately constructed from the creep curve obtained at $\sigma = -86,450$ psi.

As a final experimental result, an indication of the creep hardening behavior of alpha uranium was obtained. One tensile creep specimen was allowed to creep for 217 hours at a stress of 70,450 psi before the stress was increased to 86,450 psi. A second tensile creep specimen was allowed to creep at a stress of 78,450 psi before the stress was increased to 82,450 psi. A noticeable decrease in the creep rate from that which would have otherwise resulted was observed. The decreases in creep rates are shown in Table 3, where $\dot{\epsilon}_T$ is the tensile creep rate obtained by loading the

Table 3. Creep hardening effect in alpha uranium at room temperature

σ psi	σ_L psi	$\dot{\epsilon}_T$ min ⁻¹	$\dot{\epsilon}_T$ min ⁻¹	% reduction in $\dot{\epsilon}_T$
82,450	78,450	2.869×10^{-6}	1.022×10^{-6}	188
86,450	70,450	4.552×10^{-5}	3.900×10^{-6}	915

specimen immediately to the desired stress, and σ_T' is the tensile creep rate obtained by first creeping at the lower stress σ_L before increasing the stress to the desired σ . It is seen that by allowing alpha uranium to creep at a lower stress for awhile, a much lower creep rate at the higher stress results than would otherwise be obtained.

The fact that the time scales for both types of creep are so greatly different, as well as the fact that $\epsilon_T > \epsilon_F$ and $\dot{\epsilon}_T > \dot{\epsilon}_F$ are strong evidence that the mechanisms of creep must be different in the two cases. This suggests the possible existence of a stress-dependent dimensionless quantity, a property of the material, which relates the time scales for both types of creep.

B. The Ratio Curves

When the ratio of the tensile creep strain to the flexural creep strain for the same stress is plotted against time (Figs. 13-15), a most striking result is exhibited, as the "ratio curve" for 82,450 psi (Fig. 14) shows. The curve has the form of a standard creep curve with a well defined linear region. Thus, throughout this region, the rate of change of ϵ_T/ϵ_F with time is a constant, and has the value of 0.030 hour⁻¹ for the stress under consideration. If it were possible to predict this constant from the properties of the material, then ϵ_F could easily be calculated from ϵ_T . At a

stress of 78,450 psi, this slope has a value of 0.033 hour^{-1} , and at 86,450 psi it is 0.094 hour^{-1} .

The ratio curves for each of the three stresses all show a region of linear dependence on time. Since this result is so different from what is to be expected from previous results, an attempt to show this linear dependence theoretically for a material such as alpha uranium is imperative.

The selection of equation 14 as a mathematical model for creep lead to equation 16:

$$R(t) = \frac{\epsilon_T(t)}{\epsilon_F(t)} = \frac{C_T + D_T(1 - e^{-q_T t}) + G_T t}{C_F + D_F(1 - e^{-q_F t}) + G_F t} \quad (18)$$

as the most general expression for the ratio curve. The ratio curves shown in Figs. 13-15 are in the time range from the start of the test until the beginning of the third stage of tensile creep. For this range, the $G_F t$ term in the denominator of equation 18 can be dropped, since the flexural creep curves exhibit no second stage characteristics. As a second simplification, the origin of the creep curves can be translated C_F units in the ϵ_T / ϵ_F direction, thereby eliminating the constant term C_F in the denominator. All other constants will now be primed to account for this translation. Thus,

$$R = \frac{C'_T + D'_T(1 - e^{-q'_T t}) + G'_T t}{D'_F(1 - e^{-q'_F t})} \quad (19)$$

This can now be written:

$$R = \frac{C_T^i}{D_F^i} \frac{1}{(1 - e^{-q_F t})} + \frac{D_T^i (1 - e^{-q_T t})}{D_F^i (1 - e^{-q_F t})} + \frac{G_T^i t}{D_F^i (1 - e^{-q_F t})} \quad (20)$$

The first term on the left side varies from a value of infinity at $t = 0$ asymptotically to a constant value of C_T^i/D_F^i with increasing t . In evaluating the nature of the second term, use is made of the experimental result that $q_T \gg q_F$, where q is the parameter that determines the rate of rise per unit time of the first stage portion of the creep curve. Then the term

$$\frac{1 - e^{-q_T t}}{1 - e^{-q_F t}}$$

may be approximated by

$$\frac{1}{1 - e^{-q_F t}}$$

for t sufficiently greater than zero, since $(1 - e^{-q_T t})$ approaches unity for q_T and t large. Thus, equation 20 can be written

$$R \approx \frac{1}{D_F^i (1 - e^{-q_F t})} [(C_T^i + D_T^i) + G_T^i t] \quad (21)$$

Since $\frac{1}{(1 - e^{-q_F t})}$ is approximately a constant value over

the time range considered, it is seen that equation 21 is of the form,

$$R(t) = Q + St \quad (22)$$

where

$$Q = \frac{C_T' + D_T'}{D_F'(1 - e^{-q_F t})} \quad (23)$$

and

$$S = \frac{G_T'}{D_F'(1 - e^{-q_F t})} \quad (24)$$

Thus, an approximately linear portion of the ratio curve has been demonstrated for a material whose tensile and flexural creep behavior is similar to that of alpha uranium.

Another aspect of the ratio curves that warrants theoretical analysis is the dependence of the slope of the linear region on the applied stress. To determine how this slope varies with stress, the values of G_T' and D_F' obtained from equation 15 are substituted into equation 24. Then,

$$S = \frac{B_T' \sigma^{\beta_T}}{K_F' \sigma^{\alpha_F} (1 - e^{-q_F t})} \quad (25)$$

where the primes recall the translation of the axes that was made previously. Thus,

$$S = \frac{B_T'}{K_F'(1 - e^{-q_F t})} \sigma^{\beta_T - \alpha_F} \quad (26)$$

From equation 26 it is seen that the slope of the ratio curve increases or decreases with stress depending on whether the ratio β_T/α_F is greater than or less than one, respectively. Unfortunately, it is not possible to isolate these experimental constants, and an empirical approach to the problem is required.

C. The Prediction Equation

It would appear that the disadvantage of the ratio curve as a means of predicting flexural creep strain from the tensile creep strain is the fact that it is only valid for the range of the tensile creep curve, which corresponds to only a small part of the transient region of the flexural creep curve. The question arises whether the ratio curve can be used to predict long-time flexural creep strains. A prediction equation will now be derived which predicts the long-time flexural creep from tensile creep and ratio curve data with an accuracy of less than 10% for the maximum time achieved in testing at a stress of 82,450 psi.

A tensile creep curve and a ratio curve whose linear portions are extended beyond the third stage region out to where the flexural creep curves are undergoing second stage creep are shown in Figs. 16 and 17.

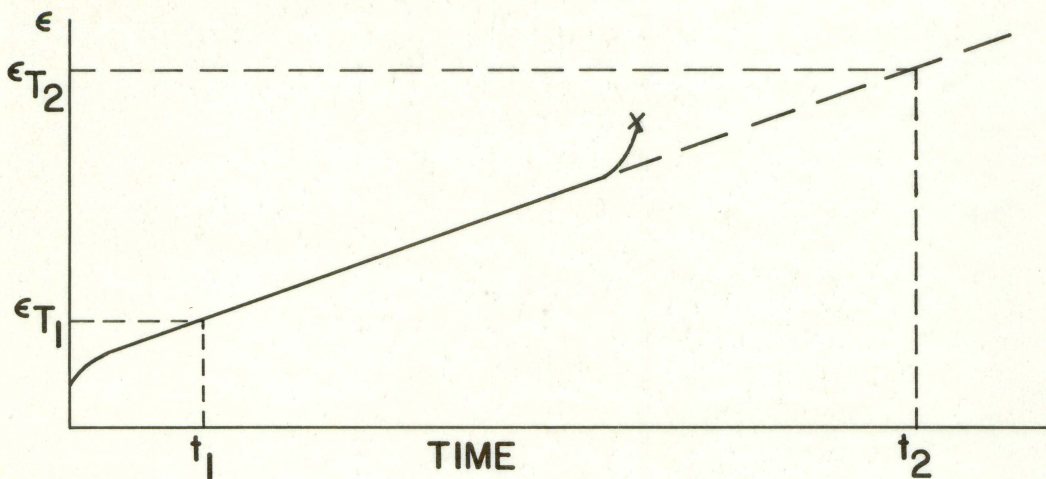


Fig. 16. A typical tensile creep curve

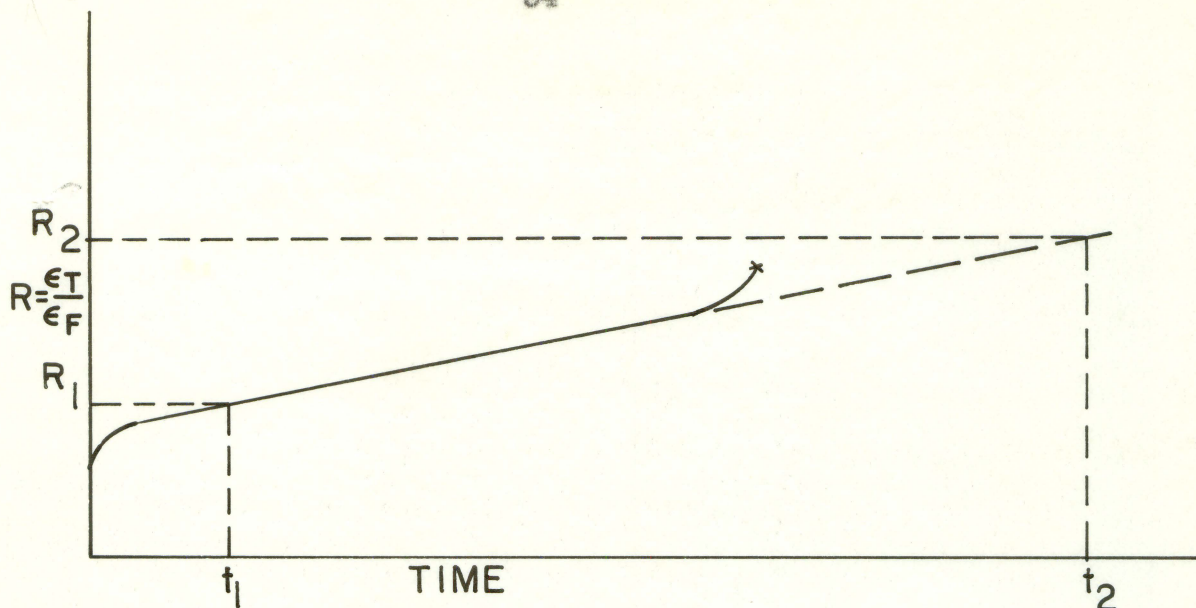


Fig. 17. A ratio curve

A time t_1 is selected, which is in the linear region of both curves, corresponding to which ϵ_{T_1} and R_1 are known. It is desired to determine ϵ_{F_2} for any time t_2 . From Fig. 16,

$$\frac{\epsilon_{T_2} - \epsilon_{T_1}}{t_2 - t_1} = \frac{d\epsilon_T}{dt}$$

the known tensile creep rate which is a constant. Thus,

$$\epsilon_{T_2} = \epsilon_{T_1} + \frac{d\epsilon_T}{dt} (t_2 - t_1) \quad (27)$$

where ϵ_{T_2} is, of course, an extrapolated creep strain. At time t_2 ,

$$R_2 = \frac{\epsilon_{T_2}}{\epsilon_{F_2}}$$

where R_2 is an extrapolated ratio. Thus,

$$\epsilon_{F_2} = \frac{\epsilon_{T_2}}{R_2} = \frac{1}{R_2} \left[\epsilon_{T_1} + \frac{d\epsilon_T}{dt} (t_2 - t_1) \right] \quad (28)$$

From the ratio curve, it is seen that

$$R_2 = R_1 + \frac{dR}{dt} (t_2 - t_1) \quad (29)$$

Substituting equation 29 into equation 28, there results

$$\epsilon_{F_2} = \frac{\epsilon_{T_1} + \frac{d\epsilon_T}{dt} (t_2 - t_1)}{R_1 + \frac{dR}{dt} (t_2 - t_1)} \quad (30)$$

Equation 30 shows that if $d\epsilon_T/dt$ and dR/dt are known, and an arbitrary t_1 selected for which ϵ_{T_1} and R_1 are known, then ϵ_{F_2} can be found for any time t_2 .

This prediction equation has been found to be highly successful in predicting the long-time flexural creep strains from the tensile creep data obtained in the experimental phase of this study. For example, for a stress of 82,450 psi, an arbitrary t_1 of 78 hours was selected, corresponding to which $\epsilon_{T_1} = 0.0787$ inches per inch and $R_1 = 17.23$. Using the experimentally determined values of 2.87×10^{-6} inches per inch per minute for the tensile creep rate, and a dR/dt of 0.030 hour^{-1} , calculated values of long-time flexural creep strains were made which agreed very well with experimental values. At a t_2 of 2442 hours, for example, the flexural creep strain was calculated to be 5510 micro-inches per inch, compared with the experimentally determined value of 5054 micro-inches per

inch, a percentage difference of 9.04. This percentage difference increases slightly with time due to the fact that the flexural creep rate is continually decreasing, whereas a linear region was assumed in the derivation of the prediction equation.

Thus, the assumptions leading to equation 30 appear to be valid, and this equation enables values of the long time flexural creep strain to be calculated which agree very well with the experimental results.

VIII. SUMMARY AND CONCLUSIONS

Tensile and flexural creep tests were carried out on alpha uranium in order to compare the creep behavior of this material under the two types of stress states. It was observed that the forms of the creep curves are vastly different. This difference may be summarized as follows:

1. The time scales of the creep curves are markedly different. The duration of both transient and second stage creep are much longer in flexural creep.
2. The tensile creep curves show a well defined linear range. The flexural creep curves exhibit a creep rate which continually decreases with time.
3. The magnitude of the tensile creep strain is greater than that of the flexural creep strain at corresponding stresses and times.
4. The second stage flexural creep rates are much smaller than the second stage tensile creep rates for corresponding values of stress.

The difference in the characteristics of the creep curves suggests that the mechanism of creep may be different in each case. A tensile creep specimen may be considered as an isolated "fiber" creeping under a constant stress. A beam undergoing flexural creep is composed of many fibers subjected to a steep stress gradient, so that the creep of any fiber may be

affected by interaction with adjacent fibers.

Although the creep curves do not have the same characteristics, the redistributed stresses in the beam may still be calculated in the conventional way, according to equation 8. This is because the exponent n in the creep rate-stress power law, $\dot{\epsilon} = B\sigma^n$, is large, for plastic and semi-plastic materials, and so the stress redistribution is fairly insensitive to changes in n .

An idea of how the creep hardening phenomenon can be used to reduce the creep rate at a stress is illustrated by the data in Table 3.

When the ratio of the tensile creep strain to the flexural creep strain was plotted against time, the resulting curve had the shape of a creep curve with a well defined linear region. This result is much different than that which would be expected if the curves were of the same form. In this case, the "ratio curve" would be a decreasing function of time. It has been found that the slope of this ratio curve, if it could be theoretically determined, would be the link by which the flexural creep strain could be calculated from tensile creep data for a material such as alpha uranium. Even though the ratio curve "exists" for just the duration of the tensile creep curve, which corresponds to only a small region in the transient part of the flexural creep curve, it was still useful in predicting long-time flexural creep strains which agreed very well with experimental values.

IX. TOPICS FOR FURTHER INVESTIGATION

The results reported in this study suggest many topics to be further investigated. Much concentrated experimental and theoretical work should be done to determine the difference between the mechanisms of creep in tension and flexure. Why are the tensile and flexural creep characteristics of alpha uranium so markedly different? The possibility of finding a stress dependent, dimensionless parameter, a function of the material, which will relate the time scales for the two types of creep should be fully explored.

The discovery of the ratio curve affords a challenging analytical and experimental study. How can the slope of the ratio curve be predicted as a function of stress for a given material? Further experimental correlation between tensile and flexural creep strains for many more stresses should be obtained.

Answers to the questions raised by the results of this study will greatly advance the present state of knowledge of the creep phenomenon.

X. LITERATURE CITED

1. Sandmeier, H. A. The kinetics and stability of fast reactors with special consideration of nonlinearities. U. S. Atomic Energy Commission Report ANL-6104 Argonne National Lab., Lemont, Ill. June, 1959.
2. Thalgot, F. W. Fast reactor safety; EBR-1. Fast Reactor Information Meeting Proc. 1947:68-76.
3. McCullough, G. H. An experimental and analytical investigation of creep in bending. Journal of Applied Mechanics, Trans. Am. Soc. Mech. Eng. 55:55-60. 1933.
4. Tapsell, H. J. and A. E. Johnson. An investigation of the nature of creep under stresses produced by pure flexure. Institute of Metals Journal 35:121. 1935.
5. Marin, J. and L. E. Zwissler. Creep of aluminum subjected to bending at normal temperatures. Proc. Am. Soc. Test. Mat. 40:937. 1940.
6. Marin, J. and G. Cuff. Creep-time relations for polystyrene under tension, bending, and torsion. Proc. Am. Soc. Test. Mat. 49:1158-1174. 1949.
7. Findley, W. N. Comments on creep and damping properties of polystyrene. Journal of Applied Physics 21:258. 1950.
8. Gohn, G. R. Discussion. Proc. Am. Soc. Test. Mat. 49:1175-1178. 1949.
9. Popov, E. P. Bending of beams with creep. Journal of Applied Physics 20:251-256. 1949.
10. Pao, Y. H. and J. Marin. Deflections and stresses in beams subjected to bending and creep. Journal of Applied Mechanics, Trans. Am. Soc. Mech. Eng. 74:478-484. 1952.
11. Findley, W. N. and J. J. Poczatek. Prediction of creep-deflection and stress distribution in beams from creep in tension. Journal of Applied Mechanics, Trans. Am. Soc. Mech. Eng. 77:165-171. 1955.
12. Finnie, I. and Heller, W. Creep of Engineering Materials. New York, N. Y., McGraw-Hill Book Co., Inc. 1959.

13. Bach, C. and R. Baumann. Elastizität und Festigkeit. 9th ed. Berlin, J. Springer. 1911.
14. Danofsky, Richard, Ames, Iowa. Data from flexural creep experiments on a beam of alpha uranium. Private communication. 1959.
15. Murphy, Glenn. Advanced Mechanics of Materials. 1st ed. New York, N. Y., McGraw-Hill Book Co., Inc. 1946.
16. Goodey, W. J. Creep deflexion and stress distribution in a beam. Aircraft Eng. 30:170-172. 1958.
17. Hoff, N. J. Approximate analysis of structures in the presence of moderately large creep deformations. Quarterly of Applied Mathematics 12:49-55. 1954.
18. Lewis, R. W. The tensile properties of metals in the inelastic range of stress. Unpublished M. S. Thesis. Ames, Iowa, Library, Iowa State University of Science and Technology. 1954.
19. Merckx, K. R. A model of mechanical behavior evaluated with creep tests applied to alpha uranium. U. S. Atomic Energy Commission Report HW-40494 Hanford Atomic Products Operation, Richland, Wash. November 17, 1955.
20. Holden, A. N. Physical Metallurgy of Uranium. Reading, Mass., Addison-Wesley Publishing Co., Inc. 1958.
21. American Society for Testing Materials. Selected A.S.T.M. Standards for Students in Engineering. Philadelphia, Pa., Author. 1943.
22. Perry, C. C. and H. R. Lissner. The Strain Gage Primer. New York, N. Y., McGraw-Hill Book Co., Inc. 1955.

XI. ACKNOWLEDGEMENTS

Most sincere appreciation is extended to Dr. Glenn Murphy, Head of the Department of Nuclear Engineering, for his continued support and helpful guidance throughout this project.

Appreciation is also expressed to the members of Nuclear Engineering Group I and in particular to Jack Bohn for their aid and suggestions during the investigation.

The tests were conducted with the materials and facilities of the Ames Laboratory.